Desalination and Water Treatment
www.deswater.com

doi: 10.1080/19443994.2015.1137492

57 (2016) 23666–23674
October

Taylor & Francis
Taylor & Francis Group

Adsorption of two microcystins onto activated carbon: equilibrium, kinetic, and influential factors

Shumin Zhu[a], Didi Yin[a], Naiyun Gao[a,*], Shiqing Zhou[a], Zhaochun Wang[b], Zhengde Zhang[b]

[a]*State Key Laboratory of Pollution Control and Resource Reuse, Tongji University, Shanghai 200092, China, Tel. +86 21 65982691; Fax: +86 21 65986313; email: gaony2014@163.com (N. Gao)*
[b]*Yixing Jiubin Waterworks, Wuxi 214200, Jiangsu Province, China*

Received 23 March 2014; Accepted 28 December 2015

ABSTRACT

Microcystins (MCs) are very stable toxins in water bodies and can be poorly removed by traditional drinking water treatment processes. Powder-activated carbon (PAC) was employed in the present study for removal of two commonly and widely occurring algal toxins, microcystin-LR (MC-LR), and microcystin-RR (MC-RR), which were obtained from cyanobacterial blooms. Results indicated that wood PAC has better adsorption capacity on MCs compared with shell and coal PAC. The Freundlich adsorption model can better describe the adsorption behavior of MCs onto PAC. And the pseudo-second-order kinetic model can better fit the adsorption process of MCs onto PAC. Moreover, the adsorption of MCs onto wood PAC was affected by temperature, pH, and anions. The adsorption rates increased with the decreasing temperature. And the adsorption capacity of wood PAC for MCs decreased with the increasing pH. Four kinds of anion hindered the adsorption and reduced the removal rate by 14–24%. Therefore, our study provides valuable information to address the water quality issues caused by microcystins, including selection of the most efficient PAC.

Keywords: Microcystins; Powder-activated carbon; Temperature; pH; Anions

1. Introduction

Activated carbon is porous carbonaceous matter which mainly takes wood, coal, and husk as raw materials and is produced after a series of physical and chemical processes including carbonization, activation, and post-processing. Due to irregular arrangement of crystallite carbon in the structure and pores between the cross connection, tissue defects can be produced during the activation, further developing the pore structure of activated carbon, resulting in a specific surface area larger than 1,500 m^2 g^{-1}. Activated carbon has strong adsorption capacity for the organic matter with relative molecular mass between 500 and 3,000 Da [1]. According to its shape, activated carbon can be divided into powdered activated carbon, granular activated carbon, and activated carbon fiber.

In recent years, cyanobacterial blooms have increasingly occurred worldwide in various water sources due to an excessive supply of nutrients [2]. In cyanobacterial bloom, harmful substances such as

---

*Corresponding author.

cyanotoxins can be released into surrounding waters during the cell growth or lysis [3]. In all toxins, microcystin-LR (MC-LR) and microcystin-RR (MC-RR) are the most commonly and widely studied. The microcystins (MCs) are highly hepatotoxic and can cause serious liver disease [4]. Moreover, a provisional safety guideline of 1.0 μg L^{-1} MC-LR in drinking water has been regulated by the World Health Organization (WHO) [5].

Generally, MCs are very stable toxins in the water bodies and poorly removed by traditional water treatment processes (such as coagulation, sedimentation, and filtration) [5]. The relative molecular mass of MC-RR and MC-LR were 1,038 and 995 g mol^{-1}, respectively. The structural characteristics and physicochemical characteristics of activated carbon suggest that activated carbon has good adsorption for MCs. The treatment with granular-activated carbon as adsorbent is stable, and is often applied in water treatment, but its price is relatively expensive, leading to the high cost of processing. Besides, granular-activated carbon filter is easy to breed bacteria, produce nitrite. Contrast to granular-activated carbon, powdered-activated carbon (PAC) has good adaptability for short-term and emergency pollution. It was reported that PAC is often used in treatment plants for the mitigation of taste and odors problem as it is relatively inexpensive and can be applied only when required [6]. Therefore, it is suitable for water treatment in sudden accidents especially when the water quality is deteriorated [7]. In the past decades, many studies have described the powdered-activated carbon adsorption for microcystin removal from water [8–11]. However, there has been little information about the microcystins elimination from algae blooms water by PAC adsorption. It is important to remove a range of microcystins by PAC in drinking water supplies since cyanobacterial blooms frequently occurred worldwide, especially in China. In this study, two microcystins (MC-LR and MC-RR) separated from algae blooms of Taihu Lake were selected as target comtaminants and algal organic matters were used to simulate the water components in real water. The results of this study can be applied to respective drinking water treatment plants (DWTPs) and provide water authorities valuable information to control microcystins, including selection of the most efficient PAC.

Three kinds of PAC were used to remove MC-LR and MC-RR obtained from cyanobacterial blooms in this study. The overall objectives of this study were: (1) to investigate the adsorption isotherms of MCs by PAC made of the wood, coal, and shell; (2) to study the adsorption kinetics of MCs onto PAC; (3) to evaluate the effect of temperature, pH, and anions on the adsorption of MCs onto PAC.

2. Materials and methods

2.1. Materials

All chemicals were at least of analytical grade except as noted. Methanol and Trifluoroacetic acid were obtained from Sigma–Aldrich (USA). Microcystins standards (MC-LR and MC-RR) were purchased from Institute of Hydrobiology, Chinese Academy of Sciences (Wuhan, China). The *Microcystis aeruginosa* cells was collected during the outbreak of cyanobacterial blooms in Wuxi District of Tai Lake, then dried and grinded into dry powder and stored at −20°C until used (Fig. S1 in Supporting Information). The characteristics of three kinds of PAC are presented in Table S1 of Supporting Information. All chemical solutions were prepared using ultrapure water produced from a Milli-Q water purification system (Millipore, USA).

2.2. Experimental procedures

Two grams of dry algal powder was dissolved into100 ml of deionized water, and magnetically stirred at room temperature for 30 min. Then the solutions were placed in a −20°C freezer for 12 h, thawed at room temperature, and frozen again. The freeze-thaw operation was repeated for three times, so that the MCs could be released thoroughly. After that, the solution was centrifuged at 5,500*g* for 10 min. The supernatant was collected, while the concentrate remained in the tube bottom was resuspended and centrifuged again as above. The supernatants from two centrifugation steps were combined, and filtered through 0.45 μm acetic acid fiber filter to remove cellular materials. The filtrate was referred to MCs extracts and the extraction liquid was blue when the extract was not further purified by solid-phase extraction (SPE).

All PAC jar tests were carried out in a batch mode in glass flasks containing 1 L MCs solution. The flasks were installed in a DKY-II constant speed rotary shaker at room temperature of 25°C and a rapid shaking speed of 160 rpm. MCs adsorption experiments were conducted where all variants were spiked into the same tests. Cook and Newcombe previously showed no competitive adsorption between the microcystin variants [10]. PAC doses ranged from 0.1 to 1.0 g L^{-1} and the spiked concentrations of MC-LR and MC-RR were 0.622 and 0.447 mg L^{-1}, respectively. If needed, solution pH was adjusted to desirable levels with NaOH and HCl. Adsorption reactions were initiated by addition of appropriate amounts of PAC. And at the same time, the blank experiment was carried out without adding PAC. At each designated sampling time, samples were collected and immediately filtered through pre-rinsed 0.45 μm acetate microporous membrane prior to analysis.

2.3. Chemical analysis

Before measurement, solid-phase extraction (SPE column, ENVI-18, Supeco) with a concentration factor of 20 was used if the MCs level in the sample was less than the detection limit (~10 μg/L). The SPE column was first activated successively by 10 mL dichloromethane and 15 mL methanol, and then washed by 20 mL Milli-Q water. Thereafter, 20 mL sample passed through the SPE at a 3 mL/min flow rate. Finally, the chromatography elute was washed out with 1.00 mL methanol and analyzed by HPLC. Recovery rates of this method ranged within 84–92% in this study.

The concentrations of MCs were quantified by a high performance liquid chromatography (HPLC), equipped with a VP-ODS column (250 mm × 4.6 mm, Shimadzu, Japan). The ultraviolet detection wavelength was set at 238 nm. The mobile phase was a mixture of ultrapure water (0.05% volume, trifluoroacetic acid) and HPLC-grade methanol (v:v = 40:60) at a flow rate of 1.0 ml min^{-1}. Injection volume was 50 μL and the column temperature was maintained at 40℃. The operation time was 10 min, the peak of MC-RR and MC-LR appeared at about 4.10 and 8.90 min, respectively.

2.4. Data analysis

The adsorption quantity was calculated according to the change of pollutant concentration before and after adsorption, as Eq. (1):

$$q_e = \frac{(C_0 - C)V}{W} \tag{1}$$

where q_e is adsorption amount (mg g^{-1}); C_0 is the initial concentration of pollutants (mg L^{-1}); C is the concentration of pollutants adsorption equilibrium (mg L^{-1}); V is volume of solution (L); W is activated carbon weight (g).

The models of Langmuir, Freundlich, and Tempkin were used to fit the adsorption isotherm curve.The three models were expressed by the Eqs. (2)–(4):

$$q_e = \frac{k_l a_l C_e}{1 + a_l C_e} \tag{2}$$

where q_e is the unit mass of activated carbon when adsorption equilibrium is reached (mg g^{-1}); C_e is the equibibrium concentration of the MCs during adsorption (mg L^{-1}); k_l is the capacity of saturated adsorption capacity (mg g^{-1}); a_l is the adsorption coefficient, equivalent to the adsorption energy for one mol solute. It is associating with the net enthalpy (L mg^{-1}):

$$q_e = k_f C_e^{\frac{1}{n}} \tag{3}$$

where k_f is the constant related with the temperature and the specific surface area of the adsorbent ($\text{mg}^{(1-1/n)}$ $\text{L}^{1/n}$ g^{-1}); n is the adsorption capacity index.

$$q_e = \frac{RT}{b} \ln(k_t C_e) \tag{4}$$

where R is the gas constant, equivalent to 8.314 J $(\text{mol K})^{-1}$; T is the absolute temperature (K); b is the Tempkin isotherm adsorption heat (J mol^{-1}); k_t is the Tempkin constant.

3. Results and discussion

3.1. Adsorption isotherms

Measured and modeled single-solute adsorption isotherm data for MC-RR and MC-LR are shown in Fig. 1. And the corresponding isotherm parameters are summarized in Table 1. Three adsorption isotherm models were evaluated in this study, including Freundlich, Langmuir, and Temkin. As shown, Langmuir model and Freundlich model can better fit the results, for the adsorption isotherms of both MC-LR and MC-RR, where the R^2 are greater than 0.95. Langmuir model assumes that the adsorption energy distributes uniform on the adsorbent surface. Freundlich is a special case of the uneven surface energy, often used to fit the granular-activated carbon adsorption on contaminants in water [12,13]. Since the surface energy of the activated carbon is not uniform, it is reasonable that the data were most consistent with the Freundlich model. From the fitting parameters listed in Table 1, the Freundlich model fitting of all the PAC have the highest R^2 greater than 0.95, where k_f value follows the descending order of wood, shell, and coal PAC. k_f represents the adsorption capacity of activated carbon in the Freundlich model. Therefore, it suggested that wood PAC exhibited better adsorption capacity on both MCs. The result is consistent with the finding of Donati et al. who reported that wood-based carbons were clearly the most effective microcystin-LR adsorbents than

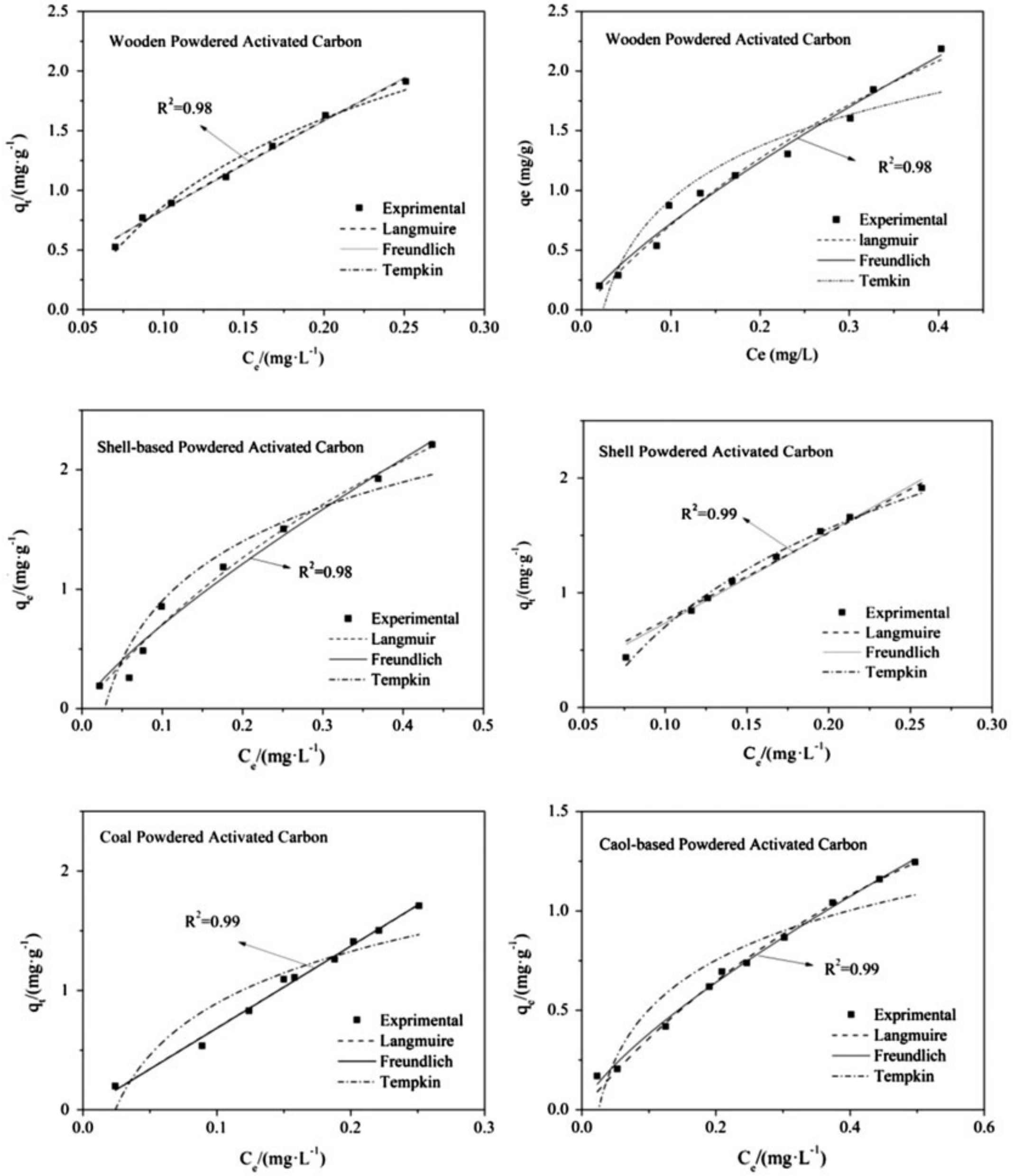

Fig. 1. Adsorption isotherm of MC-LR (left column) and MC-RR (right column) onto wood, shell, and coal based PAC. Initial conditions: PAC ranged from 0.1 to 1 g L^{-1}, $C_{\text{MC-LR}} = 0.622$ mg L^{-1} and $C_{\text{MC-RR}} = 0.447$ mg L^{-1}, temperature at 298 K, pH 7.0.

coal-based, coconut-based, and peat moss-based PACs [8]. The value of n in the Freundlich model characterizes the ascending rate of activated carbon adsorption capacity. Higher *n* value is favorable for adsorption. If the *n* value is less than 0.5, the adsorption effect on the pollutants of low concentration will be low. Generally, n values ranging between 1 and 10 will be more conducive to adsorption. In real water, the concentrations of both MCs are relatively low. Table 1 shows that the *n* values of three kinds of powder-activated carbon (PAC) were between 1 and 10, indicating that the use of activated carbon adsorption to remove MCs is feasible. The *n* value of wood PAC is higher than 2. Hence, wood PAC showed better adsorption capacity on MCs compared with the other two kinds of PAC.

3.2. *Adsorption kinetics*

It has been reported that pore volume was the main factor affecting activated carbon adsorption [14].

Table 1
Fitting parameters of adsorption isotherm model for MC-LR and MC-RR

	Carbon species	Langmuir adsorption isotherm parameters		Freundlich adsorption isotherm parameters		Tempkin adsorption isotherm parameters	
		Formula	R^2	Formula	R^2	Formula	R^2
MC-LR	Wood	$q_e = 5.00 \times [0.6 \times C_e/(1 + 0.6\ C_e)]$	0.96	$q_e = 6.97\ C_e^{1/1.1}$	0.98	$q_e = RT/0.11 \times \ln(4.19\ C_e)$	0.90
	Shell	$q_e = 4.42 \times [0.4 \times C_e/(1 + 0.4\ C_e)]$	0.80	$q_e = 6.33\ C_e^{1/0.9}$	0.99	$q_e = RT/0.10 \times \ln(3.06\ C_e)$	0.88
	Coal	$q_e = 3.19 \times [0.2 \times C_e/(1 + 0.2\ C_e)]$	0.70	$q_e = 6.13\ C_e^{1/1.9}$	0.96	$q_e = RT/0.09 \times \ln(2.28\ C_e)$	0.80
MC-RR	Wood	$q_e = 6.47 \times [1.2 \times C_e/(1 + 1.2\ C_e)]$	0.98	$q_e = 4.42\ {C_e}^{1/2.3} C_e^{1/2.3}$	0.98	$q_e = RT/0.12 \times \ln(5.28\ C_e)$	0.90
	Shell	$q_e = 5.82 \times [1.4 \times C_e/(1 + 1.4\ C_e)]$	0.98	$q_e = 4.31\ {C_e}^{1/1.3} C_e^{1/1.3}$	0.98	$q_e = RT/0.11 \times \ln(4.64\ C_e)$	0.80
	Coal	$q_e = 3.27 \times [1.2 \times C_e/(1 + 1.2\ C_e)]$	0.98	$q_e = 2.13\ C_e^{1/1.3}$	0.99	$q_e = RT/0.09 \times \ln(2.92\ C_e)$	0.90

According to Section 3.1, the treatment effect of wood PAC was better than the other two PAC. Therefore, wood PAC was selected as the efficient PAC for removing MCs in this study. The adsorption rate curve by wood PAC is represented in Fig. 2.

As seen from Fig. 2, wood PAC could effectively adsorb both MC-LR and MC-RR. It was mainly because of the low molecular mass of MCs, so that MCs can effectively be adsorbed onto microporous and mesoporous-activated carbon. In neutral conditions, the charges of MC-RR and MC-LR were between 0 and –1, respectively, and the activated carbon surface was with negative charge, so that the rejection function between two kinds of microcystins and PAC caused the difference in the adsorption effect. Therefore, wood PAC showed more efficient adsorption for MC-RR than for MC-LR.

The adsorption kinetics models of MC-LR and MC-RR onto wood PAC are shown in Fig. 3. At the beginning, the adsorption rate rose rapidly. After a period of time, the MCs absorbed onto PAC gradually reached the adsorption equilibrium, and the adsorption rate remained stable. The kinetic parameters are summarized in Table 2. The correlation coefficient R^2 of pseudo-second-order kinetic model is greater than 0.98, suggesting better fitting adsorption kinetics. Furthermore, the pseudo-second-order kinetic model comprehensively described the adsorption process of PAC adsorption of MCs, including the external liquid film diffusion, surface adsorption, and intra-particle diffusion process.

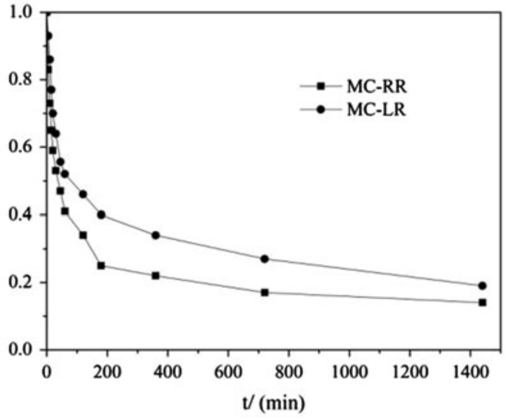

Fig. 2. Adsorption rate of MC-LR and MC-RR onto wood PAC.

3.3. Effect of temperature

The effects of different temperatures on the adsorption of MC-LR and MC-RR onto wood PAC are shown in Fig. 4. It can be seen from Fig. 4, the adsorption amounts of MCs at 15℃ are more than that at 25 and 35℃. Hence, low temperature is more preferable for adsorption. Gibbs equation and the van't Hoff equation were adopted to evaluate the effects of temperature on the equilibrium sorption (Eqs. (5)–(7)).

$$\Delta G = -RT \ln K \tag{5}$$

$$\Delta S = \frac{\Delta H - \Delta G}{T} \tag{6}$$

$$\ln K = -\frac{\Delta H}{RT} + \frac{\Delta S}{R} \tag{7}$$

where K is thermodynamic equilibrium constant; ΔG is Gibbs free energy of adsorption (kJ mol^{-1}); ΔH is the adsorption enthalpy (kJ mol^{-1}); ΔS is adsorption entropy (J (K mol)$^{-1}$).

The thermodynamic parameters for MCs adsorption at different temperature are summarized in Table 3. Von Open B determined the scope of the

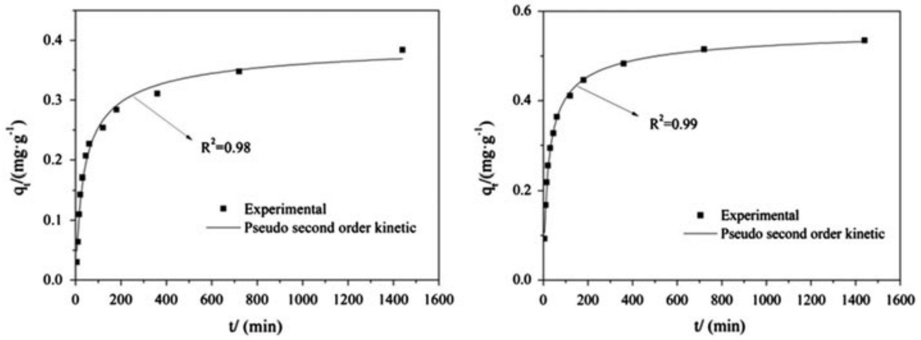

Fig. 3. Adsorption kinetic models of MC-LR (left) and MC-RR (right) onto wood PAC.

Table 2
Fitting parameters of adsorption kinetic models

	Pseudo-first-order kinetics			Pseudo-second-order kinetics		
Species	k_1 (mg g^{-1})	q_e (mg g^{-1})	R^2	k_2 (mg g^{-1})	q_e (mg g^{-1})	R^2
MCRR	0.32	0.47	0.95	0.34	0.45	0.98
MCLR	0.22	0.32	0.95	0.18	0.43	0.99

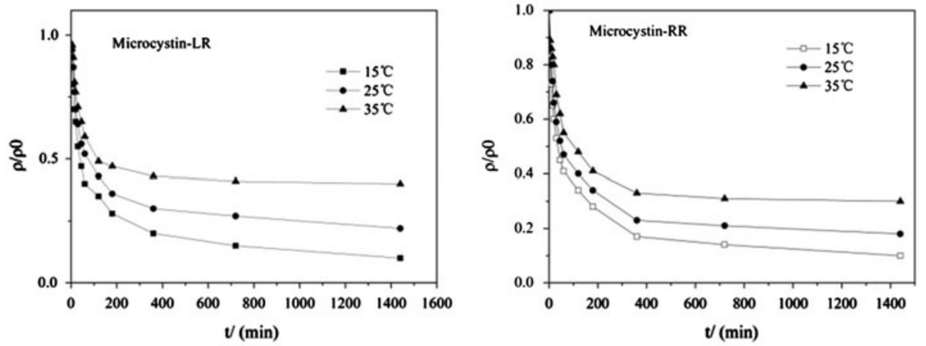

Fig. 4. Effect of temperatures on the adsorption of MC-LR and MC-RR onto wood PAC.

various forces caused by the heat of adsorption [15], and the specific data are shown in Table S2 in Supporting Information. Based on Tables 3 and S2, it was deduced that the adsorption process of MC-RR and MC-LR were dominated by physical adsorption. And the Gibbs free energy is negative, suggesting that the adsorption process of MCs is a spontaneous process. Greater value of Gibbs free energy showed stronger adsorption capacity [16]. The adsorption enthalpy changes were negative, indicating the adsorption process is exothermic in nature. Hence, low temperature would be favorable for MCs adsorption. This conclusion was consistent with the experimental results. Besides, the negative adsorption entropy value confirmed the decreased randomness of MCs molecules onto the carbon surface of PAC, attributing to some structure changes in the adsorbate and adsorbent. Therefore, it was concluded that the MCs adsorption capacities decreased as the temperature increased.

3.4. Effect of initial pH

The effects of initial pH on the adsorption of MC-LR and MC-RR onto wood PAC are shown in Fig. 5. The results showed that the adsorption capacity of wood PAC for MCs decreased with the increasing pH. Chemical analysis of the surface properties of PAC

Table 3
Thermodynamic parameters for MCs adsorption at different temperature

	T (K)	*K*	ΔG (kJ mol^{-1})	ΔH (kJ mol^{-1})	ΔS (J (K mol)$^{-1}$)
MC-RR	288	629	−15.43	−15.80	−1.4
	298	504	−15.42	−15.80	−1.4
	308	410	−15.40	−15.80	−1.4
MC-LR	288	437	−14.56	−15.60	−3.6
	298	351	−14.52	−15.60	−3.6
	308	286	−14.49	−15.60	−3.6

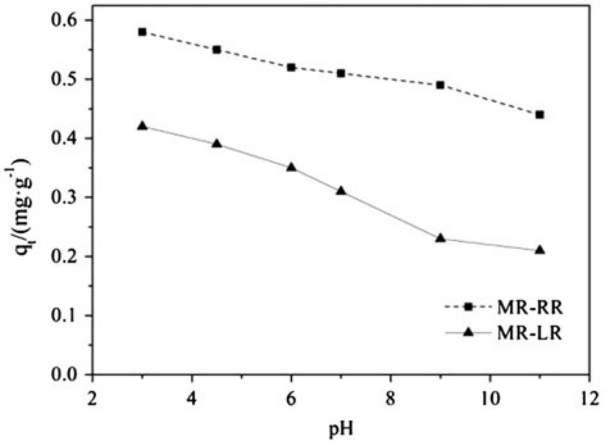

Fig. 5. Effect of initial pH on the adsorption of MC-LR and MC-RR onto wood PAC.

was conducted by using Zeta potential at different pH values. The zeta potentials of wooden PAC are presented in Fig. S2 of Supporting Information. The Zeta potential of wood PAC was negative and decreased with increasing pH value in the range of 3–11. At high pH values, the electrostatic repulsion between negatively charged MCs molecules and activated carbon played a dominant role, resulting in low PAC adsorption capacity. At low pH values, MCs molecule was electrically neutral, and electrostatic repulsion disappeared, which enhanced the adsorption of PAC.

For most of the activated carbon, the charge on the surface is negative at high pH due to the increase of hydroxyl group and anion. Moreover, the MCs also have a negative charge under basic conditions, which results in repulsion between PAC and MCs. Thus, high pH is not favorable for the activated carbon adsorption of MCs. Under acidic conditions, the weak acid functional groups in MCs will more conducive to activated carbon adsorption [17]. Furthermore, at low pH, the MCs molecules developed to huddle, and the molecular size narrowed, which increases the adsorption surface area by activated carbon. At the same time, activated carbon contained more acidic functional groups under acidic conditions. The formation of hydrogen bonds between MCs molecule and the surface of activated carbon enhanced the adsorption capacity of activated carbon [18].

3.5. Effect of anions

The effects of four ions Cl^-, NO_3^-, SO_4^{2-}, and CO_3^{2-} on the adsorption of MCs by the PAC are shown in

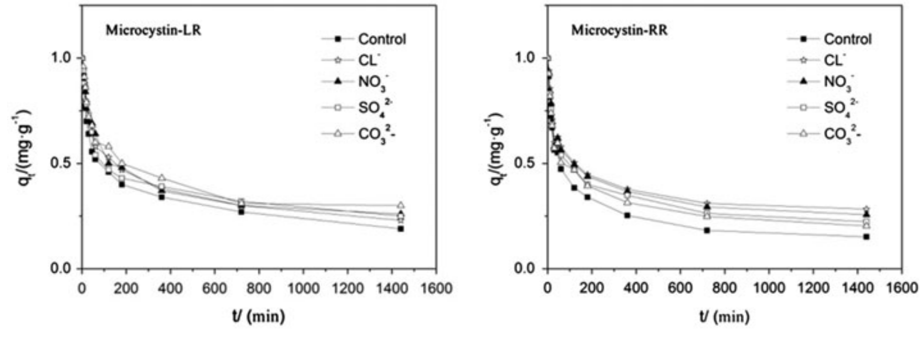

Fig. 6. Effect of anions on the adsorption of MC-LR and MC-RR onto wood PAC. Initial conditions: the concentrations of Cl^-, NO_3^-, SO_4^{2-}, and CO_3^{2-} were 10 mmol L^{-1}.

Fig. 6. It can be observed that the four ions hindered the adsorption to some degree. When Cl^-, NO_3^-, SO_4^{2-}, and CO_3^{2-} were added, the removal efficiency of MC-LR and MC-RR by wood PAC were reduced by 16, 18, 24, 16% and 14, 15, 19, 16%, respectively. It was clear that NO_3^- had the most important impact on activated carbon adsorption. Similar results were found in other study that nitrate ion had more negative effects on the adsorption capacities of perfluorohexanoic acid than sulfate and chloride ions when adsorption onto anion exchange polymers, non-ion exchange polymers and granular-activated carbon [19]. However, as the concentrations of these common anions in real water are relatively low, the coexistence of the four anions may have little effect on the removal of MCs by PAC.

4. Conclusion

(a) PAC has good efficiency for removal of MC-RR and MC-LR. The Freundlich adsorption model can better describe the adsorption behavior of MCs onto PAC. Wood PAC exhibits better adsorption capacity on MCs compared with shell and coal PAC.
(b) The pseudo-second-order kinetic model can better fit the adsorption process of MCs onto wood PAC. And wood PAC showed more efficient adsorption for MC-RR than for MC-LR.
(c) The adsorption of MCs onto wood PAC was affected by temperature, pH, and anions. The adsorption rates increased with the decreasing temperature. And the adsorption capacity of wood PAC for MCs decreased with the increasing pH. Four kinds of anion hindered the adsorption and reduced the removal rate by 14–24%.

Supplementary material

The supplementary material for this paper is available online at http://dx.doi.10.1080/19443994.2015.1137492.

Acknowledgment

This work was financially supported by the National Natural Science Foundation of China (No. 51178321, 51108327), the National Major Project of Science & Technology Ministry of China (No. 2012ZX07403-001).

References

[1] V.K. Gupta, Suhas, Application of low-cost adsorbents for dye removal—A review, J. Environ. Manage. 90 (2009) 2313–2342.
[2] X.J. Zhang, C. Chen, J.Q. Ding, A.X. Hou, Y. Li, Z.B. Niu, X.Y. Su, Y.J. Xu, E.A. Laws. The 2007 water crisis in Wuxi, China: Analysis of the origin, J. Hazard. Mater. 182 (2010) 130–135.
[3] A. Kemp, J. John, Microcystins associated with Microcystis dominated blooms in the southwest wetlands, Western Australia, Environ. Toxicol. 21 (2006) 125–130.
[4] W.W. Carmichael, Health Effects of Toxin-Producing Cyanobacteria: "The CyanoHABs", Hum. Ecol. Risk Assess. An Int. J. 7 (2001) 1393–1407.
[5] I.R. Falconer, An Overview of problems caused by toxic blue-green algae (cyanobacteria) in drinking and recreational water, Environ. Toxicol. 14 (1999) 5–12.
[6] D. Cook, G. Newcombe, P. Sztajnbok, The application of powdered activated carbon for mib and geosmin removal: Predicting pac doses in four raw waters, Water Res. 35 (2001) 1325–1333.
[7] B. Xu, T. Ye, D.P. Li, C.Y. Hu, Y.L. Lin, S.J. Xia, F.X. Tian, N.Y. Gao, Measurement of dissolved organic nitrogen in a drinking water treatment plant: Size fraction, fate, and relation to water quality parameters, Sci. Total Environ. 409 (2011) 1116–1122.
[8] C. Donati, M. Drikas, R. Hayes, G. Newcombe, Microcystin-LR adsorption by powdered activated carbon, Water Res. 28 (1994) 1735–1742.
[9] D. Cook, G. Newcombe, Removal of microcystin variants with powdered activated carbon, Water Sci. Technol. Water Suppl. 2 (2002) 201–207.
[10] D. Cook, G. Newcombe, Comparison and modeling of the adsorption of two microcystin analogues onto powdered activated carbon, Environ. Technol. 29 (2008) 525–534.
[11] L. Ho, P. Lambling, H. Bustamante, P. Duker, G. Newcombe, Application of powdered activated carbon for the adsorption of cylindrospermopsin and microcystin toxins from drinking water supplies, Water Res. 45 (2011) 2954–2964.
[12] C. Svrcek, D.W. Smith, Cyanobacteria toxins and the current state of knowledge on water treatment options: A review, J. Environ. Eng. Sci. 3 (2004) 155–185.
[13] I.A.W. Tan, B.H. Hameed, A.L. Ahmad, Equilibrium and kinetic studies on basic dye adsorption by oil palm fibre activated carbon, Chem. Eng. J. 127 (2007) 111–119.
[14] C.T. Hsieh, H.S. Teng, Influence of mesopore volume and adsorbate size on adsorption capacities of activated carbons in aqueous solutions, Carbon 38 (2000) 863–869.
[15] B. Von Oepen, W. Kördel, W. Klein, Sorption of nonpolar and polar compounds to soils: Processes, measurements and experience with the applicability of the modified OECD-Guideline 106, Chemosphere 22 (1991) 285–304.
[16] F. Yu, J. Ma, Y.Q. Wu, Adsorption of toluene, ethylbenzene and m-xylene on multi-walled carbon nanotubes with different oxygen contents from aqueous solutions, J. Hazard. Mater. 192 (2011) 1370–1379.

[17] W.J. Huang, B.L. Cheng, Y.L. Cheng, Adsorption of microcystin-LR by three types of activated carbon, J. Hazard. Mater. 141 (2007) 115–122.

[18] T. Lanaras, C. Cook, J. Eriksson, J. Meriluoto, M. Hotokka, Computer modelling of the 3-dimensional structures of the cyanobacterial hepatotoxins microcystin-LR and nodularin, Toxicon 29 (1991) 901–906.

[19] K. Wilaingam, S. Tanaka, P. Chularueangaksorn, Y. Suzuki, T. Ono, S. Fujii, Effects of anions on perfluorohexanoic acid adsorption onto anion exchange polymers, non-ion exchange polymers and granular activated carbon, Proc. Environ. Sanitary Eng. Res. 70 (2014) 65–72.